

Detecting defects in conifers with ground penetrating radar: applications and challenges

By J. R. BUTNOR^{1,6}, M. L. PRUYN², D. C. SHAW³, M. E. HARMON³, A. N. MUCCIARDI⁴ and M. G. RYAN⁵

¹Southern Research Station, USDA Forest Service, South Burlington, VT 05403, USA; ²Biological Sciences Department, Plymouth State University, Plymouth, NH, USA; ³Department of Forest Science, Oregon State University, Corvallis, OR, USA; ⁴Tree Radar, Inc., Silver Spring, MD, USA; ⁵Rocky Mountain Research Station, USDA Forest Service, Fort Collins, CO, USA;

⁶E-mail: jbutnor@fs.fed.us (for correspondence)

Summary

Our objective was to test ground penetrating radar (GPR) to non-destructively estimate decay volumes in living coniferous trees. GPR is geophysical tool which uses an antenna to propagate short bursts of electromagnetic energy in solid materials and measure the two-way travel time and amplitude of reflected signals. We compared estimates of bole decay from data collected with a SIR 3000 GPR system equipped with a 900 MHz antenna to measurements of decay from stem cross sections and increment cores for three conifer species (*Pseudotsuga menziesii*, *Thuja plicata* and *Tsuga heterophylla*). We found that near-surface decay, air-filled voids and desiccated boles had unique electromagnetic signatures, which could be separated from other defects. GPR successfully estimated the percent area of air-filled cavities and was not significantly different than results from destructive sampling. However, separation of incipient to severe decay from benign reflectors (e.g. moisture gradient between sapwood and heartwood) in conifers was much less diagnostic than with angiosperms. A limited assessment of *Acer saccharum* showed that GPR has potential to detect defects in angiosperms; however, more research is needed to outline the full range of detectable defects. Based on the trees in this study, the potential for GPR to detect decay-related defects in conifers seems limited. Despite problems detecting decay, reflections originating from the sapwood : heartwood boundary may prove useful to determine thickness of functional sapwood in conifers, but accurate quantification will require further technical development.

1 Introduction

Decomposition by wood decay fungi in living tree stems results in the destruction or decreased value of usable timber and depletion of carbon reserves in forests. Although they decrease merchantable timber value, heart rot fungi also create important habitat for wildlife and may be critical in maintaining biodiversity of natural forests (PARKS and SHAW 1996; JACKSON and JACKSON 2004; MARTIN et al. 2004). Precise methods to predict rot volume are lacking. Estimating rot volume via external visual cues (i.e. conks, broken branches, stem bulges or stem discoloration) is of limited utility because of variation caused by both species and site. Also, visual cues of rot in stems usually do not appear until the decay process is well underway. Destructive sampling of living trees provides the best assessment of physical properties including: age, moisture content, specific gravity, heartwood to sapwood ratio and an array of defects (e.g. incipient decay, wetwood, heart rot and hollowness). However, destructive or invasive sampling cannot be considered a sustainable method for early rot detection in living trees if the objective is to preserve the health of the tree.

Received: 23.6.2008; accepted: 19.11.2008; editor: S. Woodward

The prior state of the art for identifying decay in living trees with field portable equipment (not including X-ray, computed tomography (CAT) scan and nuclear magnetic resonance imaging (NMR) can be categorized as utilizing: (i) electrical sensors (TATTAR and SHIGO 1972; SHORTLE and SMITH 1987; LARSSON et al. 2004), (ii) penetrometers, e.g. Resistograph™, IML GmbH, Wiesloch, Germany (BETHGE et al. 1996; COSTELLO and QUARLES 1999), (iii) ultrasonic sensors, e.g. Arborsonic Decay Detector Fujikura Europe Ltd. Wiltshire, UK (XU et al. 2000; LEININGER et al. 2001) and the Picus Sonic Tomograph, Argus Electronics GmbH, Rostock, Germany (GILBERT and SMILEY 2004) or (iv) ground penetrating radar (GPR) (MILLER and DOOLITTLE 1990; PÉREZ-GRACIA et al. 2002; NICLOTTI et al. 2003), e.g. Tree Radar Unit, TreeRadar Inc., Silver Spring, MD, USA. Among these methods, only GPR can be considered truly non-invasive, for the others require the insertion of a drill bit or probe to make an assessment. GPR is also able to collect continuous data around the circumference of a tree.

As wood in living trees has variable electromagnetic properties (i.e. dielectric permittivity), it should be a good subject for GPR. By exploiting the electromagnetic contrast between tree roots and soil, scientists have applied GPR to map coarse root systems of trees (HRUSKA et al. 1999) and survey root system biomass over a broad range of soil conditions (BUTNOR et al. 2001, 2003; STOVER et al. 2007). Impulse propagation within wood depends on the dielectric properties of bound water, free water and cell wall components (NICLOTTI et al. 2003). Therefore, the total porosity and the total water saturation and salinity affect the radio wave propagation. Decaying wood is expected to have a different moisture content and density from sound wood and thus should also have a characteristic dielectric constant (NICLOTTI et al. 2003). MILLER and DOOLITTLE (1990) used GPR to locate knots and areas of incipient and brown rot in four different angiosperm tree species. The accuracy of the defect locations was confirmed when the trees were later felled and cut into boards. NICLOTTI et al. (2003) found that high dielectric values were well correlated with the inner decayed core of two *Platanus hybrida* Brot. Although these studies endorsed the use of the GPR for detecting the presence and extent of rot in angiosperms, both indicated the need for more extensive radar studies to further evaluate GPR's applicability to other species, such as gymnosperms.

There are two main issues that may limit the utility of using GPR to quantify wood decay. The first is whether there is sufficient electromagnetic contrast to distinguish decayed from non-decayed wood. The second is whether benign conditions such as normal moisture and density gradients, resin pockets, and heartwood formation will produce interference that prevents the delineation of defects. While GPR methodology has been available for some time, there are few published accounts evaluating its ability to detect defects in standing trees (MILLER and DOOLITTLE 1990; PÉREZ-GRACIA et al. 2002; NICLOTTI et al. 2003). In addition, these initial studies were strictly qualitative and observational and did not present quantitative data linking GPR radargrams to defects in living trees.

Our objective was to test and apply GPR to non-destructively estimate decay volumes in living coniferous trees. We selected three long-lived conifer species common in the Pacific Northwest: Douglas fir (*Pseudotsuga menziesii* Mirb. Franco), Western hemlock (*Tsuga heterophylla* Raf. Sarg.) and Western redcedar (*Thuja plicata* Don ex D. Don). Specifically, we sought to: (i) identify which decay-related defects were detectable, (ii) determine if GPR used in reflection mode could accurately define the margins of decay, (iii) identify issues that need to be considered (i.e. equipment, sampling protocol and post-collection processing) to implement GPR for heart rot surveys in these conifer species. The study involved an initial phase of scanning coupled with an intensive destructive verification followed by work at a research facility where destructive sampling was undesirable and quantification of decay would augment other studies related to carbon storage and cycling.

2 Materials and methods

The initial strategy for testing GPR to study wood decay on large conifers was two-fold: (i) Scan the base of trees with a variety of defects, fell them, scan multiple elevations of the trunk while on the ground and dissect cross-sections which corresponded with the collected radargrams, (ii) Scan multiple elevations on standing trees at the Wind River Canopy Crane site near Carson, WA using expert tree climbers and collect periodic increment cores to verify radargrams.

2.1 Study areas

Working closely with employees of Gifford Pinchot National Forest in March 2005, 10 large conifers identified as 'hazard trees' and scheduled for removal were located. Trees had one or more symptoms of disease (i.e. thinning crown, branch shedding, chlorosis) as well as physical damage from fire or basal injury. The trees were located in the North Fork Campground [Cowlitz Valley Ranger District (CVRD), 46°42'N, 121°84'W, 775 m elevation] near Randle, WA and in the Wind River Experimental Forest (WREF) along Forest Service road 43 near Stabler, WA (Mt. Adams Ranger District near 45°49'13.76"N, 121°57'06.88"W, 350 m elevation). At North Fork, three *P. menziesii* aged approximately 200 years, 40–68 m height, one *T. heterophylla*, 36 m height, one *T. plicata*, 21 m height and one *P. menziesii* dead snag were selected. The trees selected at the WREF included: one *P. menziesii*, approximately 43 m height and three *T. heterophylla*, 34–43 m height.

Trees for the second phase of the study were located at the Wind River Canopy Crane Research Facility (WRCCRF, located at 45°49'13.76"N, 121°57'06.88"W, elevation 368 m). The site is situated in a 450-year-old forest in the Wind River valley of the southern Washington Cascade Range, approximately 75 km east of Portland, OR, near Carson, WA, USA and is typical of an old-growth forest west of the Cascades (SHAW et al. 2004). We selected nine trees (three of each species; *P. menziesii*, *T. heterophylla* and *T. plicata*) within the footprint of the canopy access crane. One additional tree of each species with visible signs or symptoms of bole decay was selected from outside the crane plot.

2.2 Equipment

All radargrams were collected with a SIR 3000 ground penetrating radar unit equipped with a 900 MHz center frequency antenna (Model 3101D; GSSI Inc., Salem, NH, USA). While precise resolution size is dependent on dielectric permittivity of the substrate, penetration averages 1 m in depth. The antenna is a transducer comprised of a dipole transmitter and a receiver packaged into one unit with dimensions of 8 × 18 × 33 cm, and equipped with a handle and a small survey wheel (Fig. 1). Based on tree diameter, collection parameters consisted of: (i) two-way travel time (8–21 ns) for the energy to reach the center of the tree and be reflected back to the receiver and (ii) gain settings which amplify the reflected signal. To collect data, the antenna was placed against the trunk of a tree and moved circumferentially to acquire a complete radargram of the selected trunk elevation (Fig. 1). It was important for the antenna to maintain good contact with the bark; large air gaps or operator 'wobbles' degrade the quality of the scan. In situations where a complete scan of the tree was blocked by a branch stub or a tree was on the ground and the full circumference could not be accessed, a partial scan was collected. The spring-loaded survey wheel, which maintains contact with the bark surface, was used to meter electromagnetic pulses, effectively linking data collection density to distance traveled. Every 5 mm, a reflection trace or waveform comprised of the amplitude of reflected energy and the two-way travel time was collected. These waveforms were stacked to create a radargram, which is essentially a two dimensional profile of reflection data (amplitude and

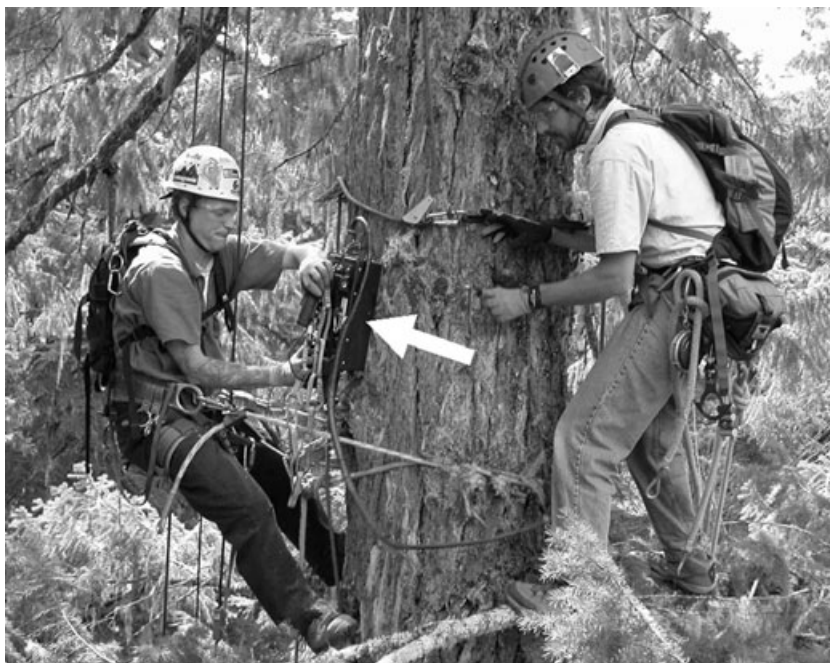


Fig. 1. Two professional tree climbers collect a circumferential scan using a 900 MHz GPR antenna equipped with a survey wheel and a SIR-3000 field computer (not visible).

depth to reflection) across a given distance. The data were recorded in standard GSSI format (*.dzt).

2.3 GPR scanning, followed by destructive sampling

Before felling, boles were marked starting 30 cm above the tree base at four to seven incremental heights 30 cm apart, then scanned with radar. After felling, partial circumference scans were collected every 3–5 m along stem lengths. It was necessary to use partial scans on the downed tree because the portion contacting the ground was not accessible. Once the scanning was complete, approximately 10-cm thick cross-sectional disks corresponding to the scan locations were sectioned from the bole. The sapwood : heartwood boundary and the presence of: incipient decay, advanced decay or rot, wetwood, knots and/or resin pockets were visually identified, outlined with a permanent marker and photographed with a size reference. IMAGEJ software (RASBAND 1997–2004) was used to estimate bark, sapwood and heartwood area from digital photographs. If defects were present, the areas of incipient decay, advanced decay or rot, cavity and wetwood were also analyzed. The freehand drawing tool was used to trace the outline of each feature on the cross-section separately (bark, sapwood, heartwood and defects). The outlined area was filled in white, the photograph turned to grayscale, and the threshold tool isolated the filled-in area. The 'analyze particles' tool calculated area of the specific feature. A sub-sample of the disks from each bole was selected for moisture and density analysis; the more rot present in the stem, the more disks that were sampled. The sub-samples were weighed for fresh mass, dried at 60°C for 72 h, and reweighed for dry mass. Moisture content was calculated as the difference between fresh and dry mass divided by dry mass and multiplied

by 100%. Specific gravity was calculated as the segment dry mass divided by fresh volume. Sub-samples from four *P. menziesii* (8–10 heights per tree), four *T. heterophylla* (6–10 heights per tree), one *T. plicata* (8 heights) and one dead snag (2 heights) were processed. We were only permitted to cut one *T. plicata* which posed an unacceptable risk in a public campground.

2.4 GPR scanning and increment borer verification

Expert tree climbers were employed to scan 10–15 elevations per tree, and periodically collect cores with an increment borer. Working at these heights (up to 55 m) was difficult and required two climbers and one ground attendant to clear ropes. To make a measurement, one climber would start the scan and hand the antenna off to the other climber on the opposite side of the tree to make a complete scan (Fig. 1). The gondola of the crane was used to support the climbers by ferrying supplies and holding the SIR 3000 which was connected to the antenna by a 30-m cable. It usually required 4 h to profile a single tree. Depending on time constraints (afternoon winds frequently grounded the crane), 3–5 increment cores were collected per tree. The sapwood : heartwood boundary in the increment core was identified visually by a change in color or moisture in the wood and sapwood thickness was recorded. The cores were divided into outer bark, inner bark and wood. The wood was cut into 2.5 cm segments until the pith. Fresh mass, length and diameter of each segment were recorded. The segments were dried at 50°C for 48 h, and then dry mass was recorded. Core segment volumes were calculated as cylinders using the measured length and diameter dimensions. Moisture content and specific gravity were calculated as described previously.

2.5 Additional sampling of eastern trees

In previously published studies (e.g. MILLER and DOOLITTLE 1990; PÉREZ-GRACIA et al. 2002; NICOLOTTI et al. 2003), GPR had been exclusively used for evaluating angiosperm tree species (hardwood sp.). Given that the early results with the three Western conifer species were less diagnostic than reported for hardwood tree species, we rapidly surveyed additional younger and smaller trees in Charlotte, Vermont (44°16'N, 73°11'W 108 m elevation) to give context to the Western data. Fifteen vigorous *Tsuga canadensis* trees aged 50–80 (40–60 cm diameter at breast height, DBH) years were scanned at breast height and the sapwood : heartwood boundary visually verified with a core collected with an increment borer. Fifteen *Acer saccharum* trees tree aged 40–100 years (45–60 cm DBH) were scanned at breast height and visually verified with an increment borer. The sapwood : heartwood boundary in *T. canadensis* was identified as the transition from wet to dry wood. In *A. saccharum*, the transition from creamy white wood to beige or light brown wood was determined to be the boundary between heartwood and sapwood.

2.6 Processing data

All radar data were processed with Radan 6.5, a multipurpose, post-collection GPR analysis software package. The ability of GPR to accurately scale the distance from the outside of the tree to a specific reflector is dependent on relative dielectric permittivity of the stem. In angiosperms, the relative dielectric permittivity (unitless) is quite uniform, averaging 13 (Dr A. Mucciardi, unpublished data). Preliminary tests with the western conifers showed that this value seemed robust and was applied as the data were collected. To date, conifers have been little studied with the GPR and required close comparison between radar data and destructive verification. GPR data is commonly visualized as a wave with positive and negative cycles as would be viewed on an oscilloscope. The most

pertinent information is the two-way travel time to phase changes, which relate to the depth of an electrical anomaly and the relative amplitude of each cycle. Raw, unfiltered data is difficult to interpret, because of signal attenuation and amplitude loss as the energy moves through the bole and is reflected back to the bark surface. To compensate for the loss of energy, gain is added during the collection process. Post-collection data filtering was applied to standardize interpretation, by scaling the amplitude of the entire waveform to the amplitude of the front surface reflection. The front surface reflection is the first positive/negative cycle and it is usually the strongest reflection. Secondary and tertiary oscillations indicate cross coupling between the pulse and receiver dipoles. Once data are scaled, detections caused by reflecting surfaces are identified when the amplitude of a reflected signal crosses a user-defined threshold. This is a relative scale which can be changed based on whether the desired feature or condition within a bole is detectable (i.e. can be discriminated from healthy tree) and was typically 1/3 of the front surface reflection. To evaluate which features were detectable, physical data collected from tree cross-sections or increment cores were directly compared with the waveforms. This was accomplished by creating a schematic of the different features (bark, sapwood, heartwood and defect class) with the corresponding waveform diagram.

To create two dimensional area projections representative of a 'slice' of the bole at a specific elevation, the depth from the outside of the tree to the first peak above the detection threshold was exported from the linear radargram. The anomaly was mapped on a polar plot using the assumption that the outer circumference of the bark was a perfect circle. From this projection, an estimate of the percent area of the tree compromised by a defect could be obtained. We compared the radar estimate of defected area to the image analysis assessment for 78 destructively sampled cross-sectional disks. The total area of all defect categories (i.e. stain, wet wood, incipient decay, decay and air-filled cavities) estimated by GPR was compared to the area obtained with IMAGEJ software from photographs.

3 Results

3.1 Detecting normal conditions with radar

Two distinct responses of the 900 MHz frequency range to normal wood anatomy were observed in the conifers studied in this experiment. Waveforms from trees with relatively thin bark (<8 cm) were characterized by one negative peak in the bark layer and a second negative peak near the sapwood : heartwood boundary (Fig. 2a). Trees with thick bark had two closely spaced negative peaks in the bark layer, followed by a third negative peak associated with the sapwood : heartwood boundary (Fig. 2b). The thick bark response was commonly observed in *P. menziesii* whose bark layer could be up to 20 cm thick. The waveforms from healthy *T. plicata*, *T. heterophylla* and *T. canadensis* (not shown) were very similar to and well represented by those of *P. menziesii* in Fig. 2a,b. The response of the 900 MHz frequency range to healthy *A. saccharum* was quite different than observed in the conifers. *Acer saccharum* without decay possessed one negative peak at the air/bark interface and were devoid of any internal reflections despite the presence of a well-defined sapwood : heartwood boundary (Fig. 2c), which was visually identified from increment borings.

3.2 Detecting defects and decay with radar

The response of the 900 MHz frequency range to internal defects was quite complex for the conifer species studied. The prevalence of different defect types varied by species and diameter, but among the conifers, the response of GPR did not seem to be species

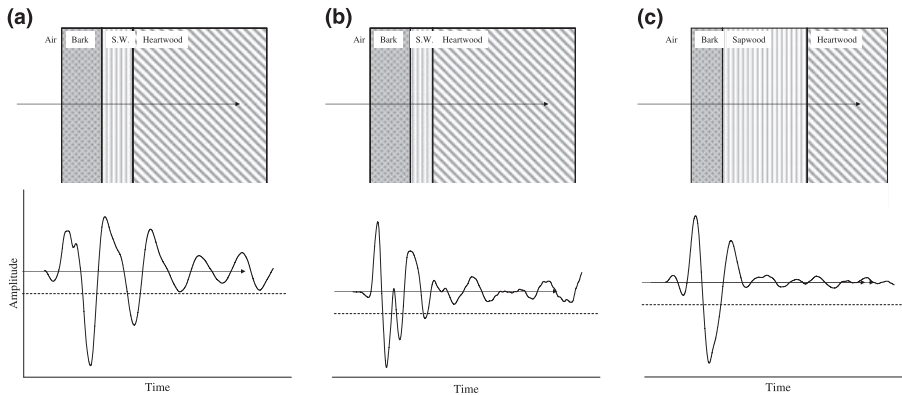


Fig. 2. Response of the 900 MHz frequency range to normal anatomy of: (a) healthy conifer with thin bark (<8 cm) (*Pseudotsuga menziesii*, WRCCF), (b) healthy conifer with thick bark (>15 cm) (*P. menziesii*, CVRD) and (c) healthy angiosperm (*Acer saccharum*, VT). The schematic diagram of anatomic features (above) corresponds to waveform diagrams (below) scaled relative to the front surface reflection. The detection threshold is represented by the dashed line.

dependent. The waveform diagrams presented are representative of the defects being compared, though there is considerable point to point variation in the specific time and amplitude values for individual trees. Severe decay or heart rot was not distinguishable from normal anatomic structures in any of the conifers in this study. For example, one large *P. menziesii* (107 cm diameter) exhibited severe heart rot encompassing more than 35% of the basal area; however this defect was not detected because it did not cross the detection threshold (Fig. 3a) and could not be discriminated from intact wood (e.g. Fig. 2b). Incipient or early stage decay was also not consistently detected in live conifers. Wetwood is a common defect in *T. heterophylla* heartwood, however, any reflection caused by wetwood was indistinguishable from the peak associated with the sapwood : heartwood boundary (Fig. 2). Analysis of cores revealed that heartwood devoid of any decay had lower moisture content than sapwood, though some *T. plicata* had layers of water soaked heartwood, which caused high amplitude reflections. These reflections were often much stronger than those associated with decay. Minor shake between annual rings was present in a few *T. canadensis* trees, but was undetectable with GPR. None of these trees possessed internal decay.

There were numerous instances where destructive interference was noted in the first negative peak (Fig. 3b) of the waveform diagram. This was caused by deep furrows or voids in the external surface of the bark (Fig. 3b) or air-filled fractures in the bark where bark sloughing was taking place. One tree had unusual sapwood decay just below the bark which similarly resulted in destructive interference. When destructive interference was present in the near-surface, detection of features deeper within the trunk was compromised, analogous to antenna decoupling from the surface of the tree (not shown).

In contrast to the negative results with decay; dry, dead wood, where the typical moisture gradient from wet sapwood to dry heartwood was less distinct or absent was readily identified in conifers. The negative peak associated with the sapwood : heartwood interface in healthy trees (Fig. 2a,b) was absent (Fig. 3c) in dry dead wood. Two *T. heterophylla* trees possessed large volumes of blue-stain fungus, were desiccated and did not exhibit a negative peak associated with the sapwood : heartwood boundary similar to *P. menziesii* (Fig. 3c). Hollows (air filled) were readily detected and characterized by multiple negative peaks which extend beyond the sapwood heartwood interface (Fig. 3d).

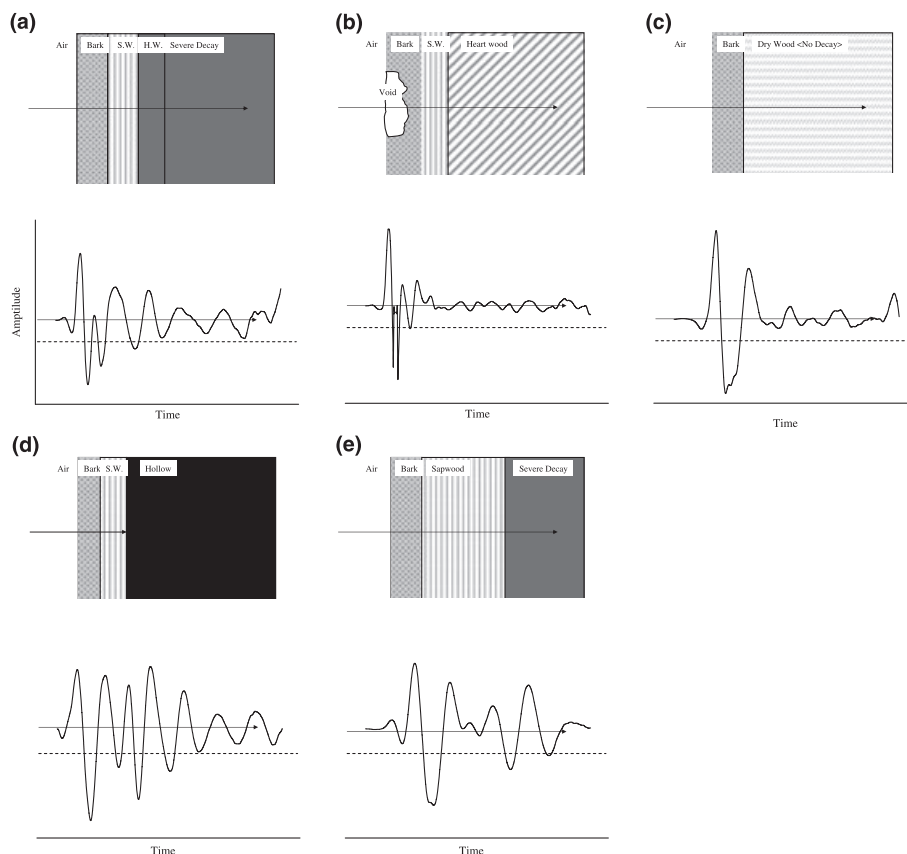


Fig. 3. Response of the 900 MHz frequency range to a variety of internal defects and decay: (a) severe heart rot (*P. menziesii*, WREF), (b) air-filled void on the outer surface of the bark (*P. menziesii*, CVRD), (c) desiccated wood with no decay (*P. menziesii*, WREF), (d) air-filled hollow (*Tsuga heterophylla*, WREF), and (e) severe decay in an angiosperm (*A. saccharum*, VT). The schematic diagram of anatomic features (above) corresponds to waveform diagrams (below) scaled relative to the front surface reflection. The detection threshold is represented by the dashed line.

The absence of any internal reflections in healthy *A. saccharum* (Fig. 2c) made it possible to consistently detect moderate to severe decay (Fig. 3e) without interference from normal anatomic features (visually verified with increment borings). The diagrams of severe to moderate decay and air-filled hollows were very similar in the distribution of peaks, but the amplitude of the reflected energy was marginally higher in the hollow *A. saccharum*. It seems unlikely that severe decay can be distinguished from hollow boles. Staining and incipient decay was not detectable in *A. saccharum*.

In Fig. 3a–e, considerable variation can be seen in the smaller peaks (right side) which follow the initial high-amplitude detection peaks (left side). These reflections are essentially background noise and so reveal little diagnostic information. The variation in amplitude in these peaks makes them seem different in the preceding figures, but it is due to variation among individual trees and different data collection and processing settings. Small diameter trees are scanned at lower time ranges and different gain settings than larger trees to compensate for signal attenuation based on tree diameter.

3.3 Estimating reflector depth

Since detection of decay was often obscured by the strong moisture gradient between sapwood and heartwood in conifers (Fig. 4a), depth to this detectable feature was used to test accuracy. Of 50 cores linked to GPR radargrams collected from standing trees at the WRCCRF, 35 were found to have strong reflections associated with depth to relatively dry

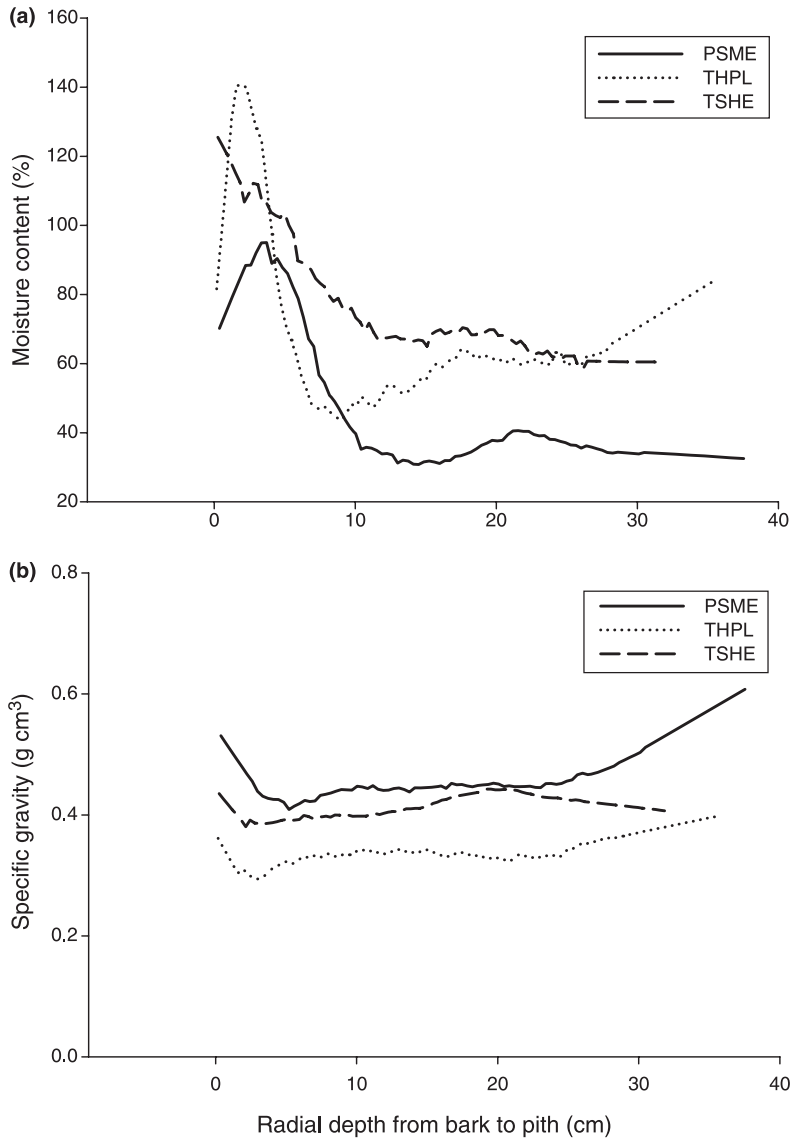


Fig. 4. Analysis of moisture content and specific gravity from healthy *P. menziesii*, *Thuja plicata* and *T. heterophylla* cores at the WRCCRF. Each line represents data for all samples collected from each species ($n = 10\text{--}13$) after applying a Gaussian negative exponential smoothing function.

heartwood, encountered at depths of 8–12 cm in healthy trees (Fig. 4a). Depth to heartwood (bark + sapwood thickness) was overestimated by 6 ± 0.7 cm (\pm SE) in *P. menziesii*, 4.6 ± 0.3 cm in *T. plicata* and 3.2 ± 0.7 cm in *T. heterophylla*. In contrast, the presence of strong reflections in the waveform diagrams was not associated with differences in specific gravity (Fig. 4b).

3.4 Decay volume accuracy

Decay volume data for all three Western conifer species was combined and analyzed with linear regression; defect area from image analysis was the independent variable, the area from GPR the dependent variable. The linear regression showed that defect area was underestimated by GPR and poorly correlated to the data from scaled photographs processed with image analysis software ($y = 0.337x + 14.0$, $R^2 = 0.22$, data not shown). When stain and wetwood were dropped from the model, the regression improved slightly (Fig. 5a). The low R^2 explained by the regression model was due to the large number of false detections caused by moisture related reflections, represented by the data points clustered at 0 on the x -axis (Fig. 5a). Since hollow trees were easily detected with GPR (Fig. 3d), Fig. 5a was reduced to only include trees with cavities. No hollow *P. menziesii* were harvested, of the 78 cross-sections, this left 19 disks from *T. plicata* and *T. heterophylla* (Fig. 5b). When considering only those trees with readily detectable cavities, there was no difference in the mean area of defect estimated by GPR (30.1%) and image analysis (35.8%).

4 Discussion

This study was principally conducted to determine if GPR could be applied to non-destructively evaluate wood decay in large conifers in old forests. Unlike angiosperms, this application of GPR in conifers does not look promising. Evidently the reflections originating from the sapwood : heartwood boundaries in living conifers are much stronger than those caused by decay, with the exception of air-filled voids. In contrast to observations with angiosperms, ground penetrating radar (900 MHz) did not detect the range of defects needed to estimate decay in living conifers. The three western conifer species that were the focus of this study displayed similar electromagnetic profiles when they possessed a strong moisture gradient associated with the sapwood (wet) and heartwood (dry). The method detected changes in moisture content, but was unable to detect changes in specific gravity. In conifers, it appears that natural moisture gradients within the tree stem often obscure the more subtle changes caused by decay.

Our findings with 15 *A. saccharum* trees, reaffirm the potential to use GPR to non-destructively identify tree defects in angiosperms (MILLER and DOOLITTLE 1990; PÉREZ-GRACIA et al. 2002; NICOLOTTI et al. 2003). Waveform diagrams of healthy *A. saccharum* resembled dead, but solid conifers. Having no internal reflections from benign conditions (i.e. a distinct sapwood : heartwood boundary) leaves more bandwidth available to detect actual defects. More work with angiosperms is needed to determine the range of detectable defects, if multiple defects can be identified and separated, if compromised basal area can be accurately mapped and if there are species-specific conditions which affect resolution.

The data for this study were not subjected to advanced signal processing algorithms. Filtering can help remove clutter from data sets, such as horizontal noise or 'ringing' and precisely locate specific point reflectors (e.g. migration). The development of filtering techniques could help improve conifer defect detection, but the fundamental problem is that the moisture gradient between normal sapwood and heartwood creates a powerful reflection. Comparing waveform diagrams of healthy and desiccated stems clearly demonstrates the influence of these gradients. This is also supported by data from

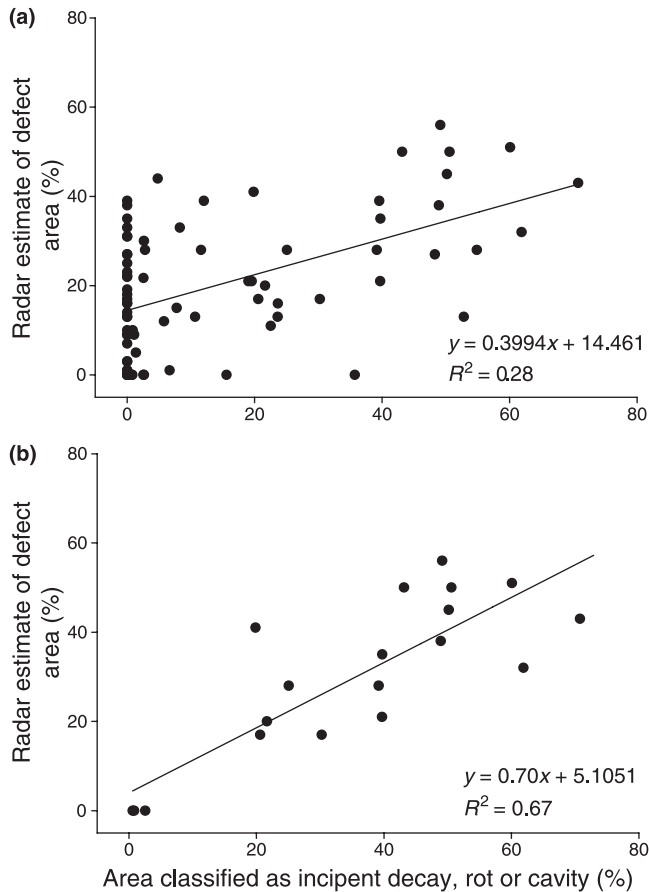


Fig. 5. Relationship between radar estimate of percent defect area and percent area classified as incipient decay, rot or cavity using image analysis for all 78 destructively sampled cross-sections from the North Fork campground and the WREF (a) and a subset of 19 cross-sections from trees with cavities at one or more elevations (b).

T. plicata, where a band of water-soaked heartwood introduced an additional negative peak in the waveform diagram. We do not have enough evidence to infer that all conifers would have similar detection problems, though it seems likely that trees with similar anatomical structure to those studied would. The rapid survey of 15 healthy *T. canadensis* trees in Vermont, displayed a similar waveform pattern. The 900 MHz center frequency electromagnetic wave used in this study may not be the best energy source for nondestructive investigation of conifers and other methodologies should be considered.

Although results varied among the species, GPR shows promise for delineating the interface between sapwood and heartwood in conifers, an application we found no potential for use in the angiosperm *A. saccharum*. Conifer species tend to have greater differences between sapwood and heartwood moisture than angiosperm species (Table 1). Of all species listed in the USDA Forest Service, Wood Handbook (ANONYMOUS 1999), *T. plicata* possessed the wettest sapwood (249%) and the greatest difference between sapwood and heartwood moisture contents (191%). *Pseudotsuga menziesii* and

Table 1. Moisture content of sapwood (SW) and heartwood (HW) of 20 North American tree species adapted from USDA Forest Service, Wood Handbook (ANONYMOUS 1999).

Scientific name	Common name	Moisture content %		
		SW	HW	SW – HW
Angiosperms				
<i>Acer saccharum</i>	Sugar Maple	72	65	7
<i>Betula alleghaniensis</i>	Yellow Birch	72	74	–2
<i>Betula papyrifera</i>	Paper Birch	72	89	–17
<i>Carya cordiformis</i>	Bitternut Hickory	54	80	–26
<i>Fagus grandifolia</i>	American Beech	72	55	17
<i>Fraxinus americana</i>	White Ash	44	46	–2
<i>Juglans nigra</i>	Black Walnut	73	90	–17
<i>Liriodendron tulipifera</i>	Yellow-poplar	106	83	23
<i>Platanus occidentalis</i>	American Sycamore	130	114	16
<i>Quercus alba</i>	White Oak	78	64	14
<i>Quercus rubra</i>	Northern Red Oak	69	80	–11
<i>Ulmus americana</i>	American Elm	92	95	–3
Gymnosperms				
<i>Picea sitchensis</i>	Sitka Spruce	142	41	101
<i>Pinus lambertiana</i>	Sugar Pine	219	98	121
<i>Pinus monticola</i>	Western White Pine	148	62	86
<i>Pinus taeda</i>	Loblolly Pine	110	33	77
<i>Pseudotsuga menziesii</i>	Douglas-Fir	115	37	78
<i>Tsuga canadensis</i>	Eastern Hemlock	119	97	22
<i>Thuja plicata</i>	Western Red Cedar	249	58	191
<i>Tsuga heterophylla</i>	Western Hemlock	170	85	85

T. heterophylla also had large moisture differentials between sapwood and heartwood compared to the range observed in other tree species (Table 1), setting the stage for a significant, yet benign (not decay related) reflection. While the moisture gradient is a strong reflector, the absolute moisture content and depth of the sapwood may also affect the presentation of a strong benign reflection. *Tsuga canadensis* presented a smaller sapwood : heartwood moisture gradient than the Western conifers, but still possessed very wet sapwood, similar to *P. menziesii* (Table 1) and exhibited moisture related reflection. Similar observations have been made in *Liriodendron tulipifera* (Dr A. N. Mucciardi, unpublished data), which has a similar sapwood : heartwood moisture profile as *T. canadensis* (Table 1), but a larger sapwood area, causing the reflections to appear closer to the pith.

One area for improvement would be to use higher frequencies to delineate closely spaced defects or affected rings. While resolution increases with frequency, the depth of penetration declines, so there is a tradeoff (CONYERS 2004; DANIELS 2004). This may be manageable in trees with diameters <60 cm where the additional penetration afforded by the 900 MHz antenna is unnecessary. Reducing the amount of energy reflected at the air/bark interface will also allow more energy to consistently transmit into the tree and reflect from internal conditions. This could be accomplished by designing antennas with curvature resembling the circumference of a tree to create a better coupling.

Our results indicated that there were species-specific effects on the estimate of depth to reflection. Depth to the sapwood : heartwood boundary was routinely overestimated with all of the western conifers, indicating that the actual relative dielectric permittivity was lower than was used. The estimate of 13 is probably a good dielectric value for general use with angiosperms, but if a high degree of accuracy is needed for anatomic investigations

(i.e. measuring sapwood volume in healthy conifers), species-specific data should be used or measured *in situ* to enhance accuracy. If trees are small enough (<50 cm diameter) and the energy from the GPR antenna can penetrate through the bole, the dielectric can be measured by putting a metallic reflector on the tree opposite the antenna and measuring the two-way travel time of the reflected energy across a known bole diameter. This calibration could then be applied to other members of the species regardless of size.

Acknowledgements

The authors would like to thank the USDA Forest Service hazard tree felling crew: Rich Brooks, Gary Deibold, Steve Hoecker and Winston Rall; and the old-growth tree climbers: James R. Dutson, Eric Baldwin, J. Blake Thomas and Kevin Hillery (Whole Tree Works, Inc.). The authors also thank the WRCCRF: Ken Bible, Chuck Campbell, Mark Creighton and Annette Hamilton for research inspiration and canopy crane services. This research was supported by a Small Grant for Exploratory Research from the National Science Foundation (DEB#0441061).

References

- ANONYMOUS, 1999: Wood Handbook: Wood as an Engineering Material, General Technical Report 113. Madison, WI: U.S. Department of Agriculture, Forest Service, Forest Products Laboratory, 463 pp.
- BETHGE, K. C.; MATTHECK, C.; HUNGER, E., 1996: Equipment for detection and evaluation of decay in trees. *J. Arboriculture* **20**, 13–37.
- BUTNOR, J. R.; DOOLITTLE, J. A.; KRESS, L.; COHEN, S.; JOHNSEN, K. H., 2001: Use of ground-penetrating radar to study tree roots in the southeastern United States. *Tree Physiol.* **21**, 1269–1278.
- BUTNOR, J. R.; DOOLITTLE, J. A.; JOHNSEN, K. H.; SAMUELSON, L.; STOKES, T.; KRESS, L., 2003: Utility of ground-penetrating radar as a root biomass survey tool in forest systems. *Soil Sci. Soc. Am. J.* **67**, 1607–1615.
- CONYERS, L. W., 2004: Ground-Penetrating Radar for Archaeology. Lanham, MD, USA: Alta Mira Press, 226 pp.
- COSTELLO, L. R.; QUARLES, S. L., 1999: Detection of wood decay in blue gum and elm: an evaluation of the Resistograph® and the portable drill. *J. Arboriculture* **25**, 311–318.
- DANIELS, D. J., 2004: Ground Penetrating Radar, 2nd edn. London, UK: The Institution of Electrical Engineers, 726 pp.
- GILBERT, E. A.; SMILEY, E. T., 2004: Picus Sonic tomography for the quantification of decay in white oak (*Quercus alba*) and hickory (*Carya* spp.). *J. Arboriculture* **30**, 277–281.
- HRUSKA, J.; ČERMÁK, J.; SUSTEK, S., 1999: Mapping tree root systems with ground penetrating radar. *Tree Physiol.* **19**, 125–130.
- JACKSON, J. A.; JACKSON, B. J. S., 2004: Ecological relationships between fungi and woodpecker cavity sites. *Condor* **106**, 37–49.
- LARSSON, B.; BENGTTSSON, B.; GUSTAFSSON, M., 2004: Nondestructive detection of decay in living trees. *Tree Physiol.* **24**, 853–858.
- LEININGER, T. D.; SCHMOLDT, D. L.; TAINTER, F. H., 2001: Using ultrasound to detect defects in trees: current knowledge and future needs. In: Proceedings, The First International Precision Forestry Cooperative Symposium. June 17–20, 2001. Seattle, Washington: College of Forest Resources, University of Washington, pp 99–107.
- MARTIN, K.; AITKEN, K. E. H.; WIEBE, K. L., 2004: Nest sites and nest webs for cavity-nesting communities in interior British Columbia, Canada: nest characteristics and niche partitioning. *Condor* **106**, 5–19.
- MILLER, W. F.; DOOLITTLE, J. A., 1990: The application of ground-penetrating radar to detection of internal defect in standing trees. In: Proceedings of the 7th International Nondestructive Testing of Wood Symposium, September 27–29, 1990. Pullman, Washington: Washington State University, pp 263–274.
- NICOLOTTI, G.; SOCCO, L. V.; MARTINIS, R.; GODIO, A.; SAMBUELLI, L., 2003: Application and Comparison of three tomographic techniques for the detection of decay in trees. *J. Arboriculture* **29**, 66–78.
- PARKS, C. G.; SHAW, D. C., 1996: Death and decay: a vital part of living canopies. *Northwest Sci.* **70**, 46–53.

- PÉREZ-GRACIA, V.; LORENZO, H.; DIAZ-PENÁLVER, N., 2002. Forestry applications of radar remote sensing with sensors In-situ. In: Proceedings of the ForestSAT Symposium, Heriot Watt University, August 5–9, 2002. Roslin: Forest Research, Northern Research Station (CD-ROM).
- RASBAND, W. S., 1997–2004: ImageJ. Bethesda, Maryland, USA: National Institutes of Health. Available at <http://rsb.info.nih.gov/ij/>. (Accessed June 2006).
- SHAW, D. C.; FRANKLIN, J. F.; BIBLE, K.; KLOPATEK, J.; FREEMAN, E.; GREENE, S.; PARKER, G., 2004: Ecological setting of the Wind River old-growth forest. *Ecosystems* **7**, 427–439.
- SHORTLE, W. C.; SMITH, K. T., 1987: Electrical properties and rate of decay in spruce and fir wood. *Phytopathology* **77**, 811–814.
- STOVER, D. B.; DAY, F. P.; BUTNOR, J. R.; DRAKE, B. G., 2007: Effect of elevated CO₂ on coarse-root biomass in Florida scrub detected by ground-penetrating radar. *Ecology* **88**, 1328–1334.
- TATTAR, T. A.; SHIGO, A. L., 1972: Relationship between the degree of resistance to a pulsed electric current and wood in progressive stages of discoloration and decay in trees. *Phytopathology* **62**, 792.
- XU, Z.; LEININGER, T. D.; TAINTER, F. H.; WILLIAMS, J. G., 2000: Examination of the Arborsonic Decay Detector for detecting bacterial wetwood in red oaks. *South. J. Appl. For.* **24**, 6–10.